1049 (1976).
[5]T. E. H. Walker and J. T. Waber, J. Phys. B 6, 1165 (1973), and 7, 674 (1974).
[6]W. Ong and S. T. Manson, J. Phys. B 11, L65 (1978).
[7]N. A. Cherepkov, Phys. Lett. A66, 204 (1978).
[8]W. R. Johnson and K. T. Cheng, Phys. Rev. Lett. 40, 1167 (1978), and Phys. Rev. A 20, 978 (1979).
[9]K.-N. Huang and A. F. Starace, Bull. Am. Phys. Soc. 22, 1325 (1977).
[10]M. G. White, R. A. Rosenberg, G. Gabor, E. D. Poliakoff, G. Thornton, S. H. Southworth, and D. A. Shirley, Rev. Sci. Instrum. 50, 53 (1979).
[11]D. Dill, Phys. Rev. A 7, 1976 (1973).
[12]T. Gustafsson, Chem. Phys. Lett. 51, 383 (1977).
[13]U. Fano, Phys. Rev. 178, 131 (1969), and 184, 250 (1969).
[14]Torop, Morton, and West have reported $1.8 \leq \beta_{5s} \leq 2.0$ for a single measurement at 83 eV, well above the energy range illustrated in Fig. 1. The resulting strength parameter for the measurement at 83 eV lies between 0.9 and the parity-favored limit $s = 1.0$. See L. Torop, J. Morton, and J. B. West, J. Phys. B 9, 2035 (1976).

Supercritical Density Profiles of CO_2-Laser-Irradiated Microballoons

R. Fedosejevs,[a] M. D. J. Burgess, G. D. Enright, and M. C. Richardson
Division of Physics, National Research Council of Canada, Ottawa, Ontario K1A 0R6, Canada
(Received 3 July 1979)

Electron-density profiles up to $40n_c$ have been measured for plasmas produced on glass microballoon targets irradiated by nanosecond, CO_2-laser pulses in the intensity range 2×10^{12} to 6×10^{13} W cm^{-2}. Critical-density scale lengths of ~ 3 μm and plateau structures, including overdense bumps, have been observed. Upper-shelf densities were greater than those attributable to radiation pressure alone, possibly indicating contributions from the superthermal plasma blowoff and self-generated magnetic fields.

Previous interferometric measurements of short-pulse laser-produced plasmas have succeeded in identifying a steepening of the electron-density profile in the region of critical density.[1-3] However, these measurements have not resolved the density structure well above n_c which is of crucial importance to the understanding of energy transport in laser-plasma interactions. In this Letter we report the first interferometric measurements of such supercritical density profiles. These measurements have been made up to densities of $40n_c$ on plasmas produced by the irradiation of glass microballoons with nanosecond CO_2-laser pulses for values of $I\lambda^2$ of (2×10^{14})–(6×10^{15}) W cm^{-2} μm^2.

Self-consistent isothermal models of the plasma profile in the region of critical density, including ponderomotive effects, have been investigated analytically for both planar and spherical flow.[4-7] For values of $v_0/v_e \gtrsim 1$ these studies predict the appearance of a step discontinuity through n_c together with possible supercritical shock structures such as overdense bumps.[6,7] In this paper we present clear evidence for the existence of an overdense bump in the density profile. However, the measured density step heights and details of the profile are not in agreement with the predictions of models which consider radiation pressure effects alone.[4-7]

The experiments were performed with one beam of the COCO-II laser facility[8] using 1–38-J, 1.3-ns (full width at half maximum), laser pulses focused to a 76-μm (full width at half maximum) intensity distribution at the center of unfilled glass microballoons. The latter had diameters of 60 and 140 μm with wall thicknesses of ~ 1 μm and were supported on thin glass stalks. The electron-density profile was measured using a folded-wave-front interferometer[9] employing an $f/2$ imaging system with a resolution of < 2 μm, illuminated by a 50–150-ps, 0.53-μm probe pulse.[10] The probe time was measured from the 20% intensity point on the leading edge of the CO_2-laser pulse with peak intensity occurring at $t \sim 0.8$ ns.

A representative sample of results for low incident energies (< 3 J) is shown in Fig. 1. It shows the development of the profile from an initial sharp step and short plateau to the formation of an overdense bump and its subsequent decay into an extended plateau. In many of the interferograms, e.g., Fig. 1(g), the plasma could be seen expanding preferentially on axis towards the incident laser beam. Because of the high resolution employed the inherent inversion errors in electron densities on axis were $\pm 0.4n_c$ which did not allow the lower-shelf density to be measured. At higher energies similar structures were

© 1979 The American Physical Society

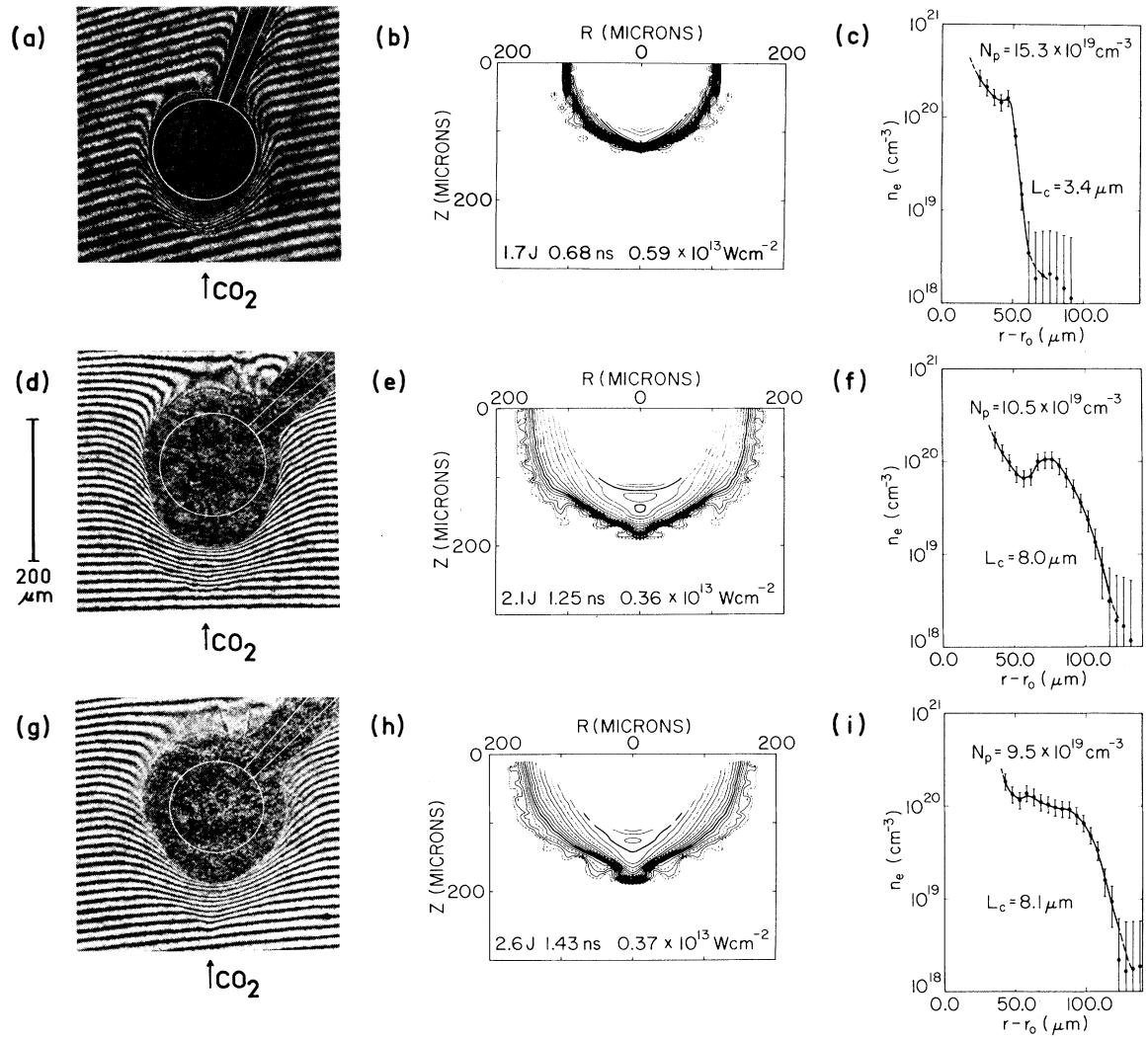

FIG. 1. (a),(d),(g) interferograms, (b),(e),(h) electron-density contour plots, and (c),(f),(i) corresponding axial electron-density profiles of the plasma produced on 140-μm-diam microballoon targets at similar energies for times of $t = 0.68$, 1.25, and 1.43 ns. The CO_2-laser beam is incident from the direction of the arrow. The energy, probe time, incident intensity, upper plateau height, and scale length at critical density are given for each shot on the axial-density profile. Evenly spaced logarithmic contour intervals are displayed with dark contours at 10^{19} and 10^{20} cm^{-3} and dotted contours at multiples of 2.5 and 5. (a) and (g) were taken probing the plasma perpendicular and parallel to the polarization of the CO_2 laser, respectively, while (d) was taken with an elliptically polarized CO_2-laser pulse.

usually present, although occasionally at energies of $\gtrsim 8$ J cratering of the profile occurred as previously observed.[2,11] Probing both parallel and perpendicular to the CO_2-laser polarization showed no significant correlation between gross plasma structure and the beam polarization.

The electron-density scale length at critical density $L_c = n_c/(dn/dx)_c$ is plotted as a function of incident laser intensity in Fig. 2. The intensity I was calculated at the critical density surface at the time of the probe pulse. The dashed line represents the scale length predicted from particle simulations by Estabrook and Kruer[12] when a Debye length of 0.086 μm, corresponding to an effective temperature of $T_{\text{eff}} = 1.3$ keV, is used. This temperature is considerably higher than the time- and space-averaged cold-electron temperature, $T_c \sim 250$ eV, deduced from x-ray spectral and continuum measurements[13-15] for nanosecond CO_2-laser pulses at 10^{13} W cm^{-2}. The predicted scaling of $L_c \propto I^{-0.48}$ is in fair agreement with the data at lower intensities reaching a minimum

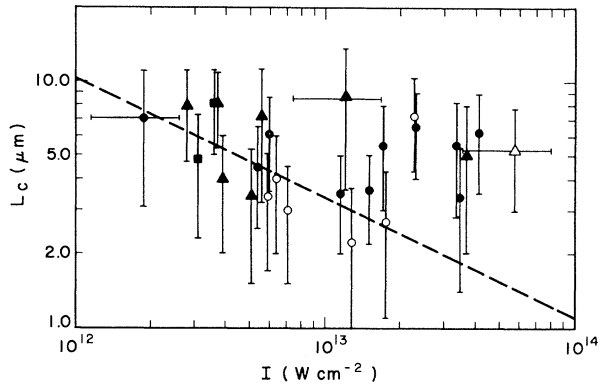

FIG. 2. Scale length vs incident intensity. Different symbols represent different polarizations of the CO_2-laser beam relative to the probe direction: perpendicular (circles), parallel (triangles), and elliptically polarized (squares). Shots before and after the peak of the CO_2-laser pulse are represented by open and closed symbols, respectively.

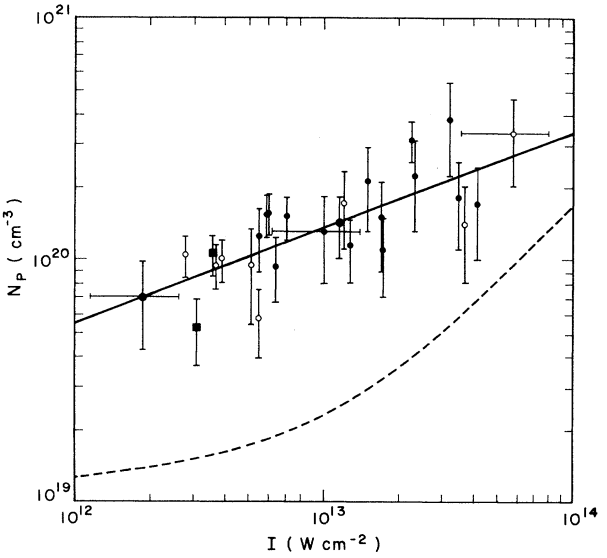

FIG. 3. Upper-density-plateau height vs incident intensity. Different symbols represent different polarizations of the CO_2-laser beam relative to the probe direction: perpendicular (closed circles), parallel (open circles), and elliptically polarized (closed squares).

value of $L_c \simeq 3.4$ μm at 10^{13} W cm^{-2} compared with the estimated resolution limit of 2–3 μm. However, at higher intensities the measured scale length appears to increase with intensity. This discrepancy could be explained by a number of factors, such as increasing $T_{\rm eff}$ near n_c, the onset of some hydrodynamic instability or nonresolvable small-scale rippling.

In some of the axial-density structures a clear overdense bump was observed [Fig. 1(f)] similar to the compressional shock transition from supersonic-to-subsonic flow predicted by Max and McKee[6] and Virmont, Pellat, and Mora.[7] The average height of the shock step was $\sim 0.3N_p$ varying from shot to shot and in some cases only an extended plateau was observed. The plateau height N_p, defined as the peak density of the density bump when observed, or the point of minimum gradient for an inclined shelf when it was not, is plotted in Fig. 3 as a function of the incident intensity. A comparison was made with the upper-shelf densities predicted by the model of Lee *et al.*[4] For a temperature of 250 eV the predicted curve, dashed line in Fig. 3, falls well below the data for which a least-squares fit gives $N_p = 13.6(I/10^{13}\ \text{W cm}^{-2})^{0.39} n_c$. This large discrepancy is not present in results obtained with 1.06-μm radiation[2,16] at similar values of $I\lambda^2$. In the present results for 10.6-μm radiation, other mechanisms must strongly influence the formation of the plasma profile.

The enhanced step height and the rounded nature of the axial electron-density profile may be partially due to the generation of fast particles and thermal-flux inhibition in the region of n_c. By including the momentum contribution from the superthermal plasma blowoff, a pressure balance can be obtained which could account for the observed density step. This may be done by using a model which includes a temperature step as well as a density step at n_c, similar to that of Estabrook, Valeo, and Kruer.[17] By integrating the one-dimensional continuity and momentum equations across the density and temperature step at n_c, the upper- to lower-shelf electron-density ratio can be obtained giving

$$\frac{n_U}{n_L} = \frac{P_L + (P_L^2 - 4v_L^2 c_U^2)^{1/2}}{2c_U^2},$$

where v_L is the lower-shelf velocity, $c_{L(U)}^2 = ZT_{L(U)}/M$ is the lower- (upper-) shelf ion acoustic velocity, P_R is the radiation pressure, and P_L is given by

$$P_L = v_L^2 + c_L^2 + ZP_R/Mn_L.$$

The temperatures of the upper and lower shelves are assumed to be the cold-electron temperature, $T_U = 250$ eV, and the hot-electron temperature,[18] $T_L = 5$ keV, respectively. By taking an ion blowoff velocity $v_L = 1.0 \times 10^8$ cm s^{-1} and lower-shelf density $n_L = 10^{18}$ cm^{-3}, an upper-shelf density of

$12n_c$ can be obtained at an intensity of 10^{13} W cm^{-2}. This value is comparable to those measured. Such a model implies a transition layer in the vicinity of critical density separating the cold-electron high-density plateau from the hot-electron low-density blowoff. The existence of such a thermal transition region would region would require a high degree of thermal-flux inhibition.

An additional factor which may significantly affect the density profile is the presence of self-generated magnetic fields, suggested by the radially confined axial expansion towards the incident laser beam observed in the interferograms. Such fields have been observed in planar-target experiments at 1 μm (Refs. 19 and 20) and inferred in those at 10 μm,[21] where the lower critical density would strengthen their role.

The authors acknowledge valuable discussions with Dr. C. Joshi, Dr. N. A. Ebrahim, and Dr. N. H. Burnett, and would like to thank Y. P. Lupien for the fabrication of microballoon targets and G. A. Berry, P. Burtyn, K. J. McKee, W. J. Orr, and R. W. Sancton for their continuing technical support. Part of this work was performed in partial fulfillment of a Ph.D. degree, University of Toronto, Canada, by one of us (R.F.).

[a]Present address: Projektgruppe für Laserforschung der Max-Planck-Gesellschaft, Garching, West Germany.

[1]R. Fedosejevs, I. V. Tomov, N. H. Burnett, G. D. Enright, and M. C. Richardson, Phys. Rev. Lett. 39, 932 (1977).

[2]D. T. Attwood, D. W. Sweeney, J. M. Auerbach, and P. H. Y. Lee, Phys. Rev. Lett. 40, 184 (1978).

[3]H. Azechi, S. Oda, K. Tanaka, T. Norimatsu, T. Sasaki, T. Yamanaka, and C. Yamanaka, Phys. Rev. Lett. 39, 1144 (1977).

[4]K. Lee, D. W. Forslund, J. M. Kindel, and E. L. Lindman, Phys. Fluids 20, 51 (1977).

[5]P. Mulser and C. van Kessel, Phys. Rev. Lett. 38, 902 (1977).

[6]C. E. Max and C. F. McKee, Phys. Rev. Lett. 39, 1336 (1977).

[7]J. Virmont, R. Pellat, and A. Mora, Phys. Fluids 21, 567 (1978).

[8]M. C. Richardson, N. H. Burnett, H. A. Baldis, G. D. Enright, R. Fedosejevs, N. R. Isenor, and I. V. Tomov, in *Laser Interaction and Related Plasma Phenomena*, edited by H. J. Schwarz and H. Hora (Plenum, New York, 1977), Vol. 4A, p. 161.

[9]R. Fedosejevs, I. V. Pomov, N. H. Burnett, and M. C. Richardson, in *Proceedings of the Twelfth International Congress on High Speed Photography, Toronto, Canada, 1–7 August, 1976* (Society of Photo-Optical Instrument Engineers, Washington, D. C.), p. 401.

[10]R. Fedosejevs and M. C. Richardson, to be published.

[11]R. Fedosejevs, M. D. J. Burgess, G. D. Enright, and M. C. Richardson, Bull. Am. Phys. Soc. 23, 768 (1978).

[12]K. G. Estabrook and W. L. Kruer, Phys. Rev. Lett. 40, 42 (1978).

[13]G. D. Enright, N. H. Burnett, and M. C. Richardson, Appl. Phys. Lett. 31, 494 (1977).

[14]C. Joshi, N. A. Ebrahim, and M. C. Richardson, to be published.

[15]H. Pepin, B. Grek, F. Rheault, and D. J. Nagel, J. Appl. Phys. 48, 3312 (1977).

[16]A. Raven and O. Willi, Phys. Rev. Lett. 43, 278 (1979).

[17]K. G. Estabrook, E. J. Valeo, and W. L. Kruer, Phys. Fluids 18, 1151 (1975).

[18]G. D. Enright, N. H. Burnett, and M. C. Richardson, J. Appl. Phys. 50, 3909 (1979).

[19]J. A. Stamper, E. A. McLean, and B. H. Ripin, Phys. Rev. Lett. 40, 1177 (1978).

[20]A. Raven, O. Willi, and P. T. Rumsby, Phys. Rev. Lett. 41, 554 (1978).

[21]N. A. Ebrahim, M. C. Richardson, R. Fedosejevs, and U. Feldman, Appl. Phys. Lett. 35, 106 (1979).

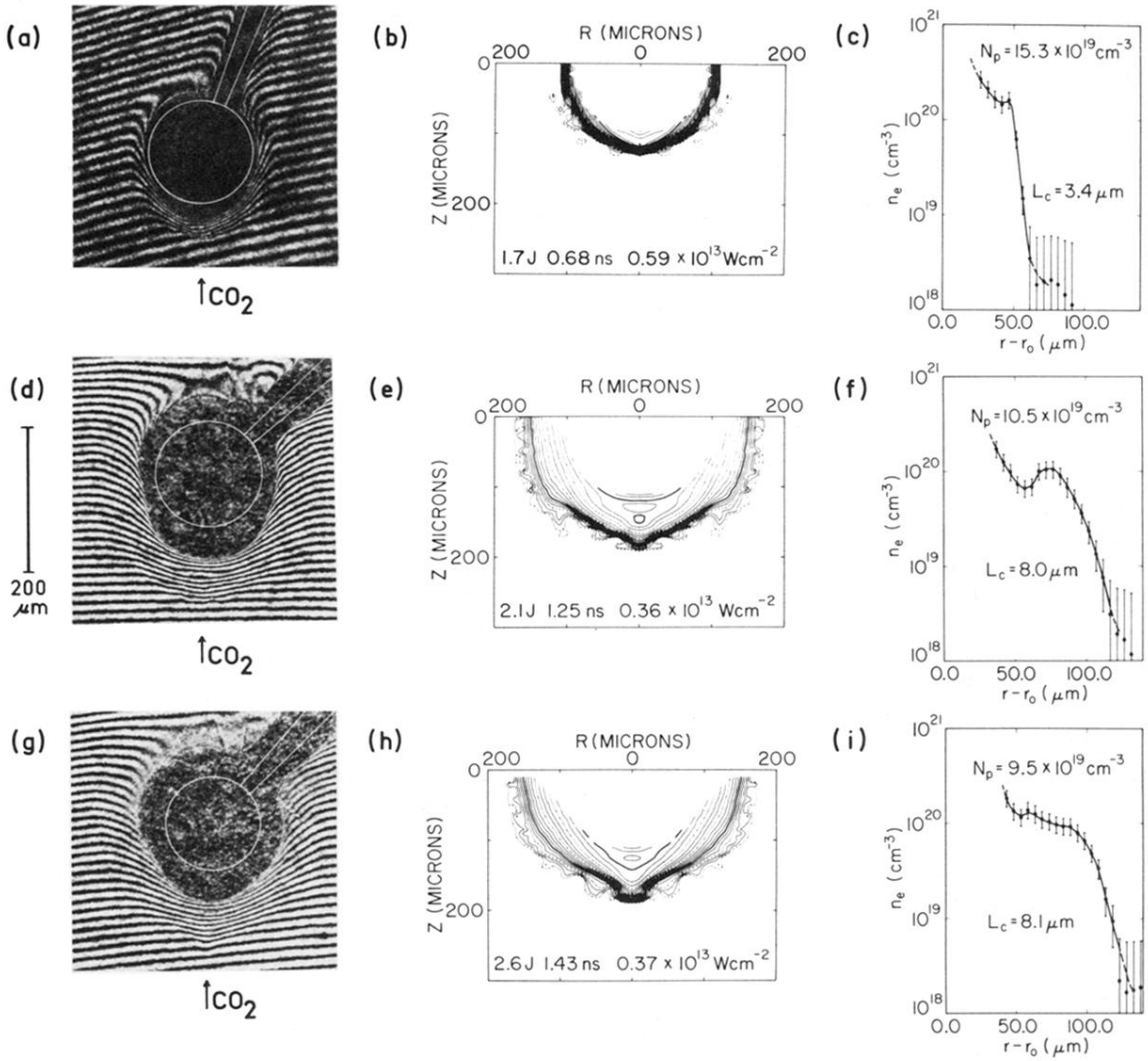

FIG. 1. (a),(d),(g) interferograms, (b),(e),(h) electron-density contour plots, and (c),(f),(i) corresponding axial electron-density profiles of the plasma produced on 140-μm-diam microballoon targets at similar energies for times of $t = 0.68$, 1.25, and 1.43 ns. The CO_2-laser beam is incident from the direction of the arrow. The energy, probe time, incident intensity, upper plateau height, and scale length at critical density are given for each shot on the axial-density profile. Evenly spaced logarithmic contour intervals are displayed with dark contours at 10^{19} and 10^{20} cm^{-3} and dotted contours at multiples of 2.5 and 5. (a) and (g) were taken probing the plasma perpendicular and parallel to the polarization of the CO_2 laser, respectively, while (d) was taken with an elliptically polarized CO_2-laser pulse.